Bulletin of Electrical Engineering and Informatics
Vol. 15, No. 6, December 2026, pp. 4979~4988
ISSN: 2302-9285, DOI: 10.11591/eei.v15i6.13373

Thermal image-based fault identification of induction motors using image features

Lakshmi Dandapani[1], Kavitha Selvaraj[2], Malathy Batumalay[3], Taqwa Hariguna[4]
[1]Department Electrical and Electronics Engineering, Faculty of Engineering and Technology, AMET Deemed to be University, Chennai, India
[2]Department of Electrical and Electronics Engineering, Easwari Engineering College, Chennai, India
[3]Faculty of Data Science and Information Technology, INTI International University, Nilai, Malaysia
[4]Master's Program in Computer Science, Faculty of Computer Science, Universitas Amikom Purwokerto, Banyumas, Indonesia

Article Info

Article history:

Received May 16, 2026
Revised Aug 27, 2026
Accepted Sep 5, 2026

Keywords:

Classification analysis
Fault diagnosis
Image feature extraction
Induction motor
Predictive maintenance
Process innovation
Thermal imaging

ABSTRACT

Three-phase induction motors are widely used in industrial systems, making reliable fault identification essential for safe and efficient operation. This study presents a non-contact thermal image-based approach for preliminary fault identification of three-phase induction motors using interpretable image features and classification analysis. Thermal images of healthy and faulty motors were acquired under different load levels and processed using hue, saturation, and value (HSV) color-space transformation, hue-based analysis, and Otsu segmentation. Five image features, namely mean, mean squared error (MSE), peak signal-to-noise ratio (PSNR), variance, and standard deviation (SD), were extracted to characterize thermal responses. The results show clear differences between healthy and faulty conditions, with faulty motors producing higher feature values and more prominent hotspots. For the four-bar rotor fault, maximum temperature increased from 26.6 °C at no load to 63.4 °C at full load. Classification performance also improved with increasing load, although overall performance remained limited. These findings demonstrate the potential of thermal imaging for non-contact induction motor condition monitoring and predictive maintenance.

This is an open access article under the CC BY-SA license.

Corresponding Author:

Taqwa Hariguna
Master's Program in Computer Science, Faculty of Computer Science, Universitas Amikom Purwokerto
Banyumas, Central Java, Indonesia
Email: taqwa@amikompurwokerto.ac.id

1. INTRODUCTION

Induction motors are widely used in industrial applications because of their robustness, reliability, and relatively low maintenance requirements. They are commonly employed in manufacturing systems, pumps, compressors, conveyors, and other rotating machinery. However, motor faults can cause overheating, abnormal vibration, efficiency degradation, unexpected downtime, and equipment failure. Early fault identification is therefore important for operational safety and maintenance efficiency. Conventional diagnosis commonly uses vibration and electrical signal analysis, including time-domain, fast Fourier transform (FFT), and wavelet transform (WT) techniques [1]–[3]. Although effective, these methods may be influenced by sensor installation, sensor location, signal quality, environmental noise, motor speed, and operating load.

Machine learning (ML) and deep learning (DL) have been increasingly applied to improve automated fault diagnosis. Convolutional neural network-long short-term memory (CNN-LSTM), fusion neural networks, CNN-based methods, deep belief networks, convolutional deep belief networks, and

autoencoder-based approaches have demonstrated potential for rotating machinery and induction motor diagnosis [4]–[15]. However, these data-driven methods generally require representative datasets, appropriate feature extraction, and robust validation to achieve reliable generalization. These requirements can be challenging when fault data are limited or operating conditions vary.

Thermal imaging provides a non-contact alternative for induction motor condition monitoring. Motor faults may increase losses, friction, or localized heating, producing changes in surface temperature distribution and thermal hotspots. Previous studies have demonstrated the feasibility of thermographic analysis [16], thermal imaging for three-phase induction motors [17], thermal mapping [18], ML-based thermal diagnosis [19], few-shot learning [20], and CNN-based thermal image analysis [21]. Unlike contact-based sensors, thermal cameras provide spatial temperature information without requiring physical sensor installation, making thermal imaging a useful complementary technique for industrial condition monitoring.

Despite these developments, several challenges remain. The performance of vibration-based diagnosis can vary with sensor configuration, speed, load, and fault type [22]–[24], while ML- and DL-based approaches can be affected by dataset size, class diversity, sensor configuration, and generalization capability [25]–[27]. Although thermal imaging has shown promising results, many studies emphasize complex feature-learning and classification methods rather than simple and interpretable thermal descriptors [28]–[30]. Recent research also highlights the need for improved robustness and generalization in image-based induction motor diagnosis [31]. In particular, further investigation is required to understand how basic image features, including mean, mean squared error (MSE), peak signal-to-noise ratio (PSNR), variance, and standard deviation (SD), differ between healthy and faulty conditions and how operating load influences thermal patterns [32].

Therefore, this study investigates a practical non-contact thermal-image-based approach for preliminary fault identification of a three-phase induction motor under no-load, 50% load, and 100% load conditions. Thermal images are processed using hue, saturation, and value (HSV) color-space transformation, hue-based analysis, and Otsu segmentation, followed by extraction of five interpretable features: mean, MSE, PSNR, variance, and SD. Torque-speed measurements are also used to provide supporting information for interpreting the thermal response under different loads. The study focuses on determining whether simple thermal image characteristics can provide useful fault-related information and how their diagnostic behavior changes with operating load. This approach is intended as a complementary monitoring method rather than a replacement for established vibration-based diagnosis and provides a basis for future validation using larger datasets, additional fault conditions, and multisensor integration.

2. METHOD

This section describes the proposed methodology for preliminary fault identification of three-phase induction motors using non-contact thermal imaging. The experimental workflow consists of five main stages: experimental setup, thermal image acquisition, image preprocessing, feature extraction, and motor condition classification [33], [34]. Torque-speed measurements are additionally recorded to provide operational information for interpreting the thermal response under different loading conditions. The overall experimental configuration is shown in Figure 1.

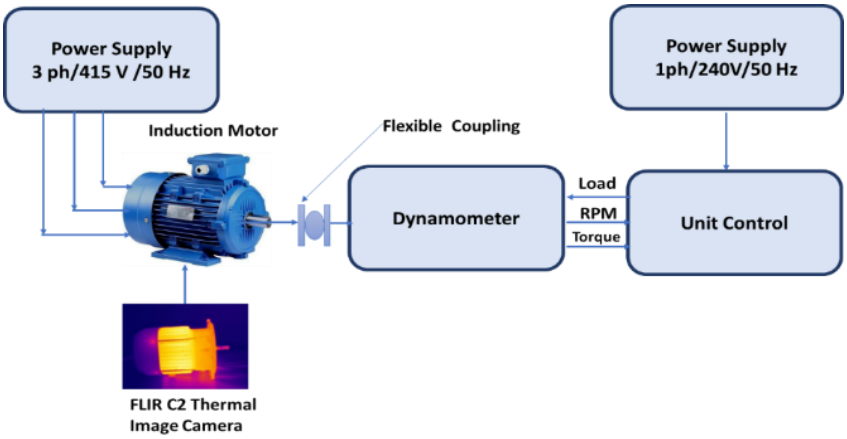


Figure 1. Overall experimental configuration

2.1. Experimental setup, data acquisition, and torque-speed measurement

The experimental setup consisted of a Clarke 80B/4 three-phase squirrel-cage induction motor, dynamometer, control panel, and forward looking infrared (FLIR) C2 thermal camera. The motor used a delta connection, operated at 50 Hz, and had a rated power of 0.75 kW (1.0 hp) and speed of 1480 rpm [35], [36]. The experimental motor is shown in Figure 2. Thermal images were acquired using a FLIR C2 camera with an infrared resolution of 80×60 pixels, visual resolution of 640×480 pixels, 9 Hz image frequency, 0.10 °C thermal sensitivity, and approximately ±2 °C measurement accuracy [37]. The camera was positioned approximately 1–2 feet from the motor and maintained at a fixed position during acquisition. Images were collected under healthy conditions and one-bar, four-bar, and eight-bar rotor faults at 0%, 50%, and 100% load [38]–[40]. The thermal camera is shown in Figure 3.

The data acquisition and control configuration is presented in Figure 4. Motor speed and torque were recorded using the dynamometer during each operating condition. Torque was calculated using (1):

$$T = 9.81 \times R \times (S_1 - S_2) \quad (1)$$

where (T) is torque (N·m), (R) is the dynamometer radius or calibration factor, (S_1) and (S_2) are the dynamometer readings. These measurements were used as supporting information for interpreting the thermal response under different load conditions.



Figure 2. Induction motor



Figure 3. Thermal camera

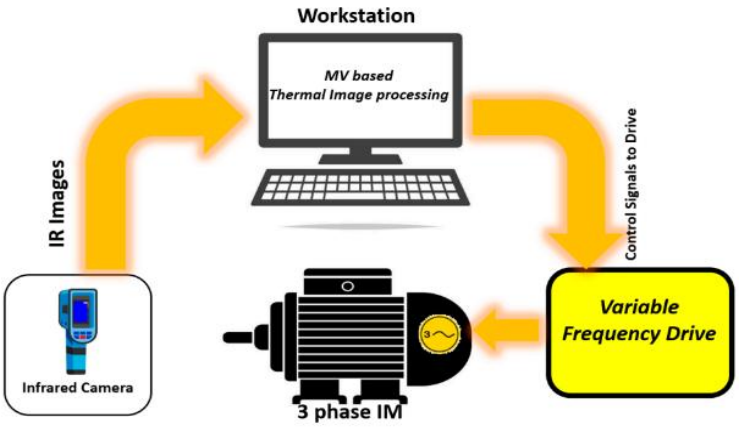


Figure 4. Data acquisition and control of induction motor

2.2. Image preprocessing and feature extraction

Thermal images were processed using MATLAB R2022b. The images were first converted into the HSV color space, and the hue component was selected to emphasize temperature-related regions. Otsu thresholding was then applied to segment the relevant thermal region from the background [41]. The same preprocessing procedure was applied to all healthy and faulty conditions under the three load levels.

The processed images were characterized using five features: mean, MSE, PSNR, variance, and SD. Mean represents the average pixel intensity, while variance and SD describe the intensity distribution within the thermal region. MSE and PSNR were used to characterize image differences [42], [43]. The extracted features were subsequently used to distinguish healthy and faulty motor conditions and support the classification process.

2.3. Classification and performance evaluation

The extracted thermal image features were used to identify healthy and faulty motor conditions. PSNR was selected as the decision indicator by comparing its value with a predefined threshold (T), as expressed in (2):

$$PSNR \leq T: fault - free\ motor\ PSNR > T: faulty\ motor \quad (2)$$

Where PSNR is the PSNR and (T) is the classification threshold. The extracted features were evaluated under 0%, 50%, and 100% load conditions to examine the effect of operating load on fault identification. Classification performance was assessed using false positive rate (FPR), precision, F1-score, and matthews correlation coefficient (MCC). These metrics were used to evaluate the ability of the proposed approach to distinguish healthy and faulty motor conditions under different loads. The resulting classification performance was interpreted together with the thermal features and torque-speed measurements to assess the relationship between motor loading and thermal fault characteristics.

3. RESULTS AND DISCUSSION

3.1. Thermal image analysis and feature extraction under different load conditions

The thermal response of the induction motor was evaluated under different rotor fault and load conditions. Figures 5–7 present the thermal analysis of the four-bar rotor fault at 0%, 50%, and 100% load, respectively. At no load, the maximum temperature was 26.6 °C, with a relatively weak and less distinguishable hotspot (Figure 5). At 50% load, the maximum temperature increased to 41.6 °C, and the hotspot became more visible (Figure 6). Under full-load operation, the maximum temperature reached 63.4 °C, producing a more prominent hotspot (Figure 7).

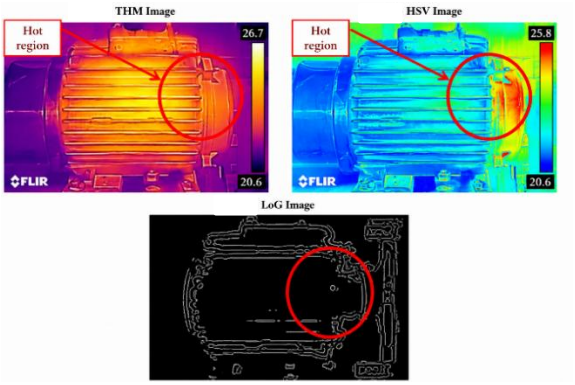


Figure 5. Analysis of thermal images for a four-bar rotor failure without any load

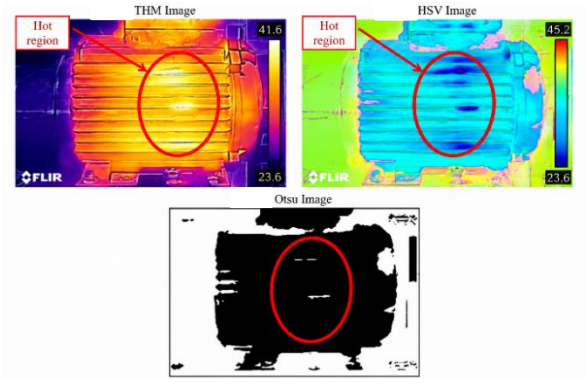


Figure 6. Analysis of thermal images for a four-bar rotor failure with 50% load

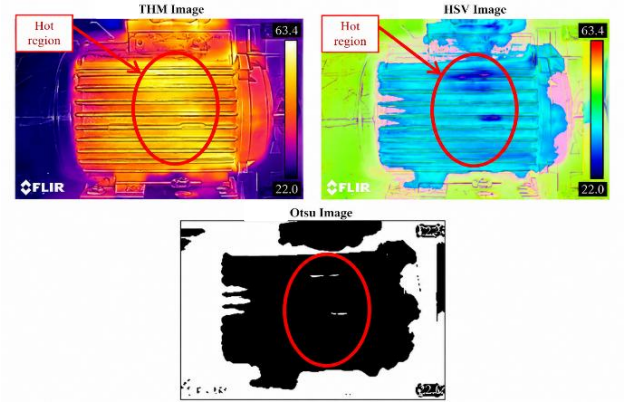


Figure 7. Analysis of thermal images for a four-bar rotor failure with 100% load

The processed thermal images were characterized using five features: mean, MSE, PSNR, variance, and SD. Table 1 presents the extracted features for healthy and faulty motor conditions. The faulty motor generally showed higher feature values than the healthy motor, indicating a clear difference in thermal characteristics. For the faulty motor, the mean increased from 0.4851 at 0% load to 0.5002 at 100% load, while MSE increased from 0.4851 to 0.5003, PSNR from 0.4849 to 0.5097, and variance from 0.4840 to 0.5012. In contrast, the healthy motor showed less consistent changes with increasing load. These results indicate that simple image features can distinguish healthy and faulty conditions, while the increasing temperature and hotspot visibility demonstrate the strong influence of operating load on the thermal response.

Table 1. Extracted image features of healthy and faulty motors

Condition	Load (%)	Mean	MSE	PSNR	Variance	SD
Healthy	0	0.0313	0.032	0.0329	0.1086	0.3419
Healthy	50	0.0341	0.0347	0.0372	0.1231	0.5305
Healthy	100	0.0246	0.1249	0.1243	0.284	0.523
Faulty motor	0	0.4851	0.4851	0.4849	0.4840	0.5389
Faulty motor	50	0.4945	0.4932	0.4921	0.4936	0.4950
Faulty motor	100	0.5002	0.5003	0.5097	0.5012	0.5572

Overall, the results show that both motor condition and operating load influence the extracted thermal features. The higher feature values and more visible hotspots under faulty and higher-load conditions suggest that thermal image characteristics can provide useful information for preliminary motor fault identification. However, the features should be interpreted together with the operating condition because the thermal response changes with load.

3.2. Classification performance and model behavior

The classification performance under different load conditions is presented in Table 2. The F1-score increased from 0.1438 at 0% load to 0.1743 at 100% load, while precision increased from 0.1444 to 0.1778 and MCC from 0.2254 to 0.2747. These improvements are consistent with the stronger thermal response observed at higher loads in Figures 5–7. However, the relatively low classification values indicate that the extracted thermal features are not yet sufficient for reliable standalone fault diagnosis.

Table 2. Average classification performance under different load conditions

Load (%)	FP rate	F1 value	Precision	MCC
0	0.1434	0.1438	0.1444	0.2254
50	0.1474	0.1476	0.1512	0.2315
100	0.1488	0.1743	0.1778	0.2747

The training and validation behavior is shown in Figure 8. Training accuracy approached 1.0 while validation accuracy remained considerably lower, and training loss decreased while validation loss increased during later epochs. This divergence indicates overfitting and limited model generalization. Therefore, the high training accuracy should not be interpreted as evidence of high diagnostic reliability. The error distribution shown in Figure 9 provides supplementary information on model behavior but does not eliminate the generalization issue observed in Figure 8.

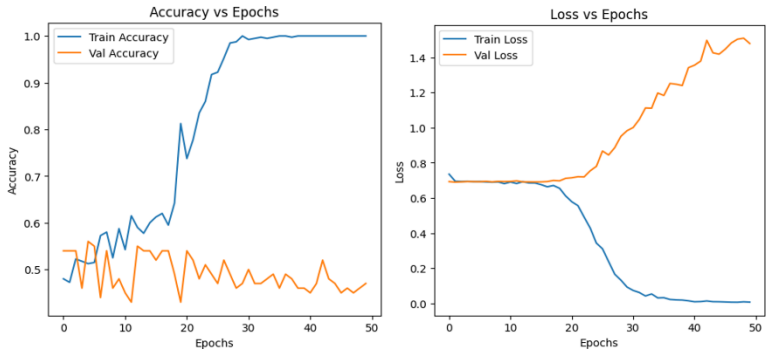


Figure 8. Accuracy and loss curves

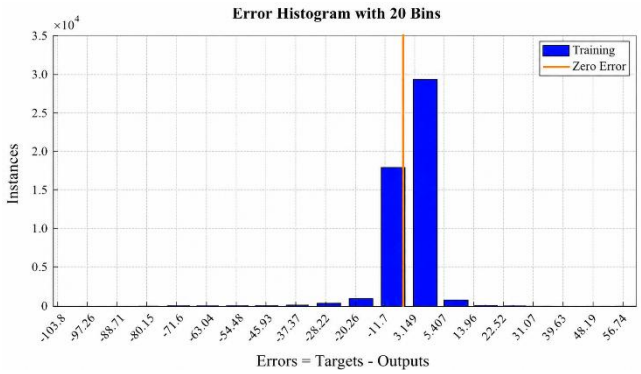


Figure 9. Error histogram of the model output

Overall, the results indicate that the proposed thermal image features contain fault-related information, particularly under higher load conditions, but further improvement is required for reliable diagnosis. Larger and more diverse datasets, independent testing, cross-validation, regularization, and additional fault and load conditions should be considered in future work.

3.6. Hotspot identification and torque-speed relation

The identified hotspot and torque-speed measurements provide additional engineering context for the thermal response. The hottest region detected in the thermal image is shown in Figure 10. The hotspot became more prominent with increasing load, consistent with the thermal feature and classification results presented in Tables 1 and 2.



Figure 10. Thermal image showing the hottest spot

The measured torque-speed relationship is presented in Table 3. As the applied load increased, motor speed decreased from 1400 to 1334 rpm, while torque increased from 0 to 15.49 N·m and current increased from 0.456 to 0.682 A. These results indicate that higher loading increased the electrical and mechanical demand on the motor and was accompanied by a stronger thermal response. Thus, the torque-speed measurements support the interpretation that operating load is an important factor affecting the observed thermal characteristics.

Table 3. Torque-speed relation

Speed (rpm)	S1	S2	I (A)	Torque T (N·m)
1400	0	0	0.456	0
1372	2.6	13	0.541	10.2
1346	6	18	0.596	11.77
1334	7.2	23	0.682	15.49

The results demonstrate a consistent relationship between increasing load, decreasing speed, increasing torque and current, and increasing thermal response. However, the reported PSNR value of

49.5116 differs substantially from the normalized PSNR values in Table 1; therefore, its calculation and relationship to the classification threshold should be clarified before it is used as an independent diagnostic criterion.

3.7. Discussion

The results demonstrate that thermal image features can distinguish healthy and faulty induction motor conditions, with faulty motors generally showing higher mean, MSE, PSNR, variance, and SD values, consistent with previous thermal-imaging studies [15], [17], [21]. Operating load strongly affected the thermal response, as the maximum temperature of the four-bar rotor fault increased from 26.6 °C at no load to 41.6 °C at 50% load and 63.4 °C at full load, accompanied by increasing torque and current and decreasing motor speed. Classification performance also improved at higher load, with F1-score, precision, and MCC increasing from 0.1438, 0.1444, and 0.2254 at no load to 0.1743, 0.1778, and 0.2747 at full load. However, the relatively low classification performance and the divergence between training and validation results indicate overfitting and limited generalization. Compared with conventional vibration monitoring, thermal imaging provides non-contact spatial temperature information and can therefore serve as a complementary monitoring technique [15], [17], [21]. Nevertheless, the results are limited by the specific motor, fault conditions, camera configuration, and load levels used in the experiment. The reported PSNR value of 49.5116 also requires clarification because it differs from the normalized values in Table 1. Future studies should use larger datasets, repeated measurements, independent testing, additional fault conditions, and multisensor integration to improve diagnostic robustness and generalization [22], [26], [27], [44].

4. CONCLUSION

This study presented a non-contact thermal image-based approach for preliminary fault identification of three-phase induction motors using image processing, interpretable feature extraction, and classification analysis. The results demonstrate measurable differences between healthy and faulty motor conditions based on MSE, PSNR, variance, and SD, with faulty motors generally exhibiting higher feature values and more prominent thermal hotspots. Operating load significantly influenced the thermal response, with the maximum temperature of the investigated four-bar rotor fault increasing from 26.6 °C at no load to 41.6 °C at 50% load and 63.4 °C at full load, accompanied by increasing torque and current and decreasing motor speed. Classification performance also improved at higher load levels, with increased F1-score, precision, and MCC; however, the relatively low performance and observed overfitting indicate that the proposed approach is not yet sufficient for reliable standalone fault diagnosis. Overall, the findings demonstrate the potential of simple and interpretable thermal image features as a complementary non-contact method for induction motor condition monitoring, particularly where direct sensor installation is inconvenient. Future research should employ larger and more diverse datasets, repeated measurements, additional fault types, independent validation, and multisensor integration combining thermal imaging with vibration, current, acoustic, or torque-speed information to improve diagnostic robustness and generalization.

FUNDING INFORMATION

This research was funded by INTI International University, Malaysia.

AUTHOR CONTRIBUTIONS STATEMENT

This journal uses the Contributor Roles Taxonomy (CRediT) to recognize individual author contributions, reduce authorship disputes, and facilitate collaboration.

Name of Author	C	M	So	Va	Fo	I	R	D	O	E	Vi	Su	P	Fu
Lakshmi Dandapani		✓	✓			✓		✓	✓					
Kavitha Selvaraj	✓	✓		✓				✓	✓		✓			
Malathy Batumalay	✓			✓	✓		✓			✓	✓	✓		✓
Taqwa Hariguna	✓	✓		✓	✓					✓		✓	✓	

C : **C**onceptualization
M : **M**ethodology
So : **So**ftware
Va : **Va**lidation
Fo : **Fo**rmal analysis
I : **I**nvestigation
R : **R**esources
D : **D**ata Curation
O : Writing - **O**riginal Draft
E : Writing - Review & **E**diting
Vi : **Vi**sualization
Su : **Su**pervision
P : **P**roject administration
Fu : **Fu**nding acquisition

CONFLICT OF INTEREST STATEMENT

Authors state no conflict of interest.

DATA AVAILABILITY

The data that support the findings of this study are available from the corresponding author upon reasonable request.

REFERENCES

[1] T. A. Putra, Yuhandri, and A. Ramadhanu, "A Modified Watershed Algorithm for Rice Plant Growth Stage Analysis," *Journal of Applied Data Sciences*, vol. 7, no. 2, pp. 833–848, May 2026, doi: 10.47738/jads.v7i2.1117.

[2] X. Chen, B. Zhang, and D. Gao, "Bearing fault diagnosis base on multi-scale CNN and LSTM model," *Journal of Intelligent Manufacturing*, vol. 32, no. 4, pp. 971–987, Apr. 2021, doi: 10.1007/s10845-020-01600-2.

[3] X. Jian, W. Li, X. Guo, and R. Wang, "Fault diagnosis of motor bearings based on a one-dimensional fusion neural network," *Sensors*, vol. 19, no. 1, p. 122, Jan. 2019, doi: 10.3390/s19010122.

[4] S. K. Gundewar and P. V. Kane, "Condition Monitoring and Fault Diagnosis of Induction Motor," *Journal of Vibration Engineering and Technologies*, vol. 9, no. 4, pp. 643–674, Jun. 2021, doi: 10.1007/s42417-020-00253-y.

[5] S. N. Venkatesh and V. Sugumaran, "Fault Detection in aerial images of photovoltaic modules based on Deep learning," in *IOP Conference Series: Materials Science and Engineering*, vol. 1012, no. 1, p. 012030, 2021, doi: 10.1088/1757-899x/1012/1/012030.

[6] C. Hernando and T. E. Sondakh, "Deep neural network framework for early detection of student depression based on academic and behavioral data," *Artificial Intelligence in Learning*, vol. 2, no. 3, pp. 194–207, 2026, doi: 10.63913/ail.v2i3.63.

[7] T. Guo, J. Dong, H. Li, and Y. Gao, "Simple convolutional neural network on image classification," in *2017 IEEE 2nd International Conference on Big Data Analysis, ICBDA 2017*, Mar. 2017, pp. 721–724, doi: 10.1109/ICBDA.2017.8078730.

[8] Z. Qiu, C. Duan, W. Yao, P. Zeng, and L. Jiang, "Adaptive Lyapunov Function Method for Power System Transient Stability Analysis," *IEEE Transactions on Power Systems*, vol. 38, no. 4, pp. 3331–3344, 2023, doi: 10.1109/TPWRS.2022.3199448.

[9] D. Sugianto and B. Priyodono, "Explainable AI for Android malware detection: Enhancing transparency, privacy, and accountability in cyberlaw," *Journal of Cyber Law*, vol. 2, no. 3, pp. 178–192, 2026, doi: 10.63913/jcl.v2i3.32.

[10] I. Arel, D. Rose, and T. Karnowski, "Deep machine learning-A new frontier in artificial intelligence research," *IEEE Computational Intelligence Magazine*, vol. 5, no. 4, pp. 13–18, Nov. 2010, doi: 10.1109/MCI.2010.938364.

[11] J. G. Alonzo, A. M. V. Abrigo, R. A. Alismo, M. A. S. Alon-alon, A. L. F. Baran, and J. O. Guballo, "Relationship of AI-powered robot servers on brand trust: The mediating role of service reliability and moderating effect of technological readiness," *Journal of Digital Society*, vol. 2, no. 3, 2026, doi: 10.63913/jds.v2i3.36.

[12] H. Shao, H. Jiang, X. Zhang, and M. Niu, "Rolling bearing fault diagnosis using an optimization deep belief network," *Measurement Science and Technology*, vol. 26, no. 11, p. 115002, Nov. 2015, doi: 10.1088/0957-0233/26/11/115002.

[13] H. Shao, H. Jiang, H. Zhang, and T. Liang, "Electric Locomotive Bearing Fault Diagnosis Using a Novel Convolutional Deep Belief Network," *IEEE Transactions on Industrial Electronics*, vol. 65, no. 3, pp. 2727–2736, Mar. 2018, doi: 10.1109/TIE.2017.2745473.

[14] S. Liu, J. Xie, C. Shen, X. Shang, D. Wang, and Z. Zhu, "Bearing fault diagnosis based on improved convolutional deep belief network," *Applied Sciences*, vol. 10, no. 18, p. 6359, Sep. 2020, doi: 10.3390/APP10186359.

[15] A. Glowacz, "Thermographic fault diagnosis of electrical faults of commutator and induction motors," *Engineering Applications of Artificial Intelligence*, vol. 121, p. 105962, May 2023, doi: 10.1016/j.engappai.2023.105962.

[16] S. M. Rajtmajer, B. Smith, and S. Phoha, "Non-negative sparse autoencoder neural networks for the detection of overlapping, hierarchical communities in networked datasets," *Chaos*, vol. 22, no. 4, Dec. 2012, doi: 10.1063/1.4771600.

[17] A. Glowacz and Z. Glowacz, "Diagnosis of the three-phase induction motor using thermal imaging," *Infrared Physics and Technology*, vol. 81, pp. 7–16, Mar. 2017, doi: 10.1016/j.infrared.2016.12.003.

[18] J. Xu *et al.*, "Stacked sparse autoencoder (SSAE) for nuclei detection on breast cancer histopathology images," *IEEE Transactions on Medical Imaging*, vol. 35, no. 1, pp. 119–130, Jan. 2016, doi: 10.1109/TMI.2015.2458702.

[19] Y. Qi, C. Shen, D. Wang, J. Shi, X. Jiang, and Z. Zhu, "Stacked Sparse Autoencoder-Based Deep Network for Fault Diagnosis of Rotating Machinery," *IEEE Access*, vol. 5, pp. 15066–15079, 2017, doi: 10.1109/ACCESS.2017.2728010.

[20] F. Zhou, T. Sun, X. Hu, T. Wang, and C. Wen, "A sparse denoising deep neural network for improving fault diagnosis performance," *Signal, Image and Video Processing*, vol. 15, no. 8, pp. 1889–1898, Nov. 2021, doi: 10.1007/s11760-021-01939-w.

[21] J. D. Pelegrin, U. J. Dreyer, J. P. Bazzo, and J. C. C. D. Silva, "Faults Diagnosis in Induction Motors through Thermal Mapping Produced by the RDTS System," *IEEE Sensors Journal*, vol. 21, no. 18, pp. 20061–20068, Sep. 2021, doi: 10.1109/JSEN.2021.3097940.

[22] M. Xia, T. Li, L. Xu, L. Liu, and C. W. De Silva, "Fault Diagnosis for Rotating Machinery Using Multiple Sensors and Convolutional Neural Networks," *IEEE/ASME Transactions on Mechatronics*, vol. 23, no. 1, pp. 101–110, Feb. 2018, doi: 10.1109/TMECH.2017.2728371.

[23] I. H. Kao, W. J. Wang, Y. H. Lai, and J. W. Perng, "Analysis of Permanent Magnet Synchronous Motor Fault Diagnosis Based on Learning," *IEEE Transactions on Instrumentation and Measurement*, vol. 68, no. 2, pp. 310–324, Feb. 2019, doi: 10.1109/TIM.2018.2847800.

[24] J. Wang, G. Wu, L. Wan, Y. Sun, and D. Jiang, "Recurrent neural network applied to fault diagnosis of underwater robots," in *Proceedings - 2009 IEEE International Conference on Intelligent Computing and Intelligent Systems, ICIS 2009*, Nov. 2009, vol. 1, pp. 593–598, doi: 10.1109/ICICISYS.2009.5357773.

[25] C.-M. Lin and E.-A. Boldbaatar, "Fault Accommodation Control for a Biped Robot Using a Recurrent Wavelet Elman Neural Network," *IEEE Systems Journal*, vol. 11, no. 4, pp. 2882–2893, Dec. 2015, doi: 10.1109/jsyst.2015.2409888.

[26] Z. Xu, G. Tang, and B. Pang, "An Infrared Thermal Image Few-Shot Learning Method Based on CAPNet and Its Application to Induction Motor Fault Diagnosis," *IEEE Sensors Journal*, vol. 22, no. 16, pp. 16440–16450, Aug. 2022, doi: 10.1109/JSEN.2022.3192300.

[27] A. Choudhary, T. Mian, and S. Fatima, "Convolutional neural network based bearing fault diagnosis of rotating machine using thermal images," *Measurement: Journal of the International Measurement Confederation*, vol. 176, p. 109196, May 2021, doi: 10.1016/j.measurement.2021.109196.

[28] H. A. Alyoubi, "Advanced Machine Learning Approaches for Predicting County-Level Electoral Outcomes within Democratic Governance Systems," *Journal of Digital Society*, vol. 2, no. 2, pp. 81–97, Jun. 2026, doi: 10.63913/jds.v2i2.26.
[29] A. A. Arul, R. Vinifa, J. A. Kumar, and N. R. Shanker, "Secondary magnetic field based runtime prediction of shaft bend in induction motor using giant magneto-resistance sensor," *Measurement: Journal of the International Measurement Confederation*, vol. 269, p. 120816, Apr. 2026, doi: 10.1016/j.measurement.2026.120816.
[30] C. Izumi and R. A. Putawa, "A Hybrid Machine-Learning and Econometric Panel VAR Approach to Assess FinTech Adoption and Digital Economy Growth in Emerging Markets," *Fintech Innovation Journal*, vol. 1, no. 1, pp. 1–16, 2025, doi: 10.63913/ftij.v1i1.10.
[31] N. Thepnuan, "Exploring Artificial Intelligence for Learning Enhancement with Predictive and Explainable Modelling," *Artificial Intelligence in Learning*, vol. 2, no. 1, pp. 17–34, Mar. 2026, doi: 10.63913/ail.v2i1.29.
[32] J. A. Kumar, N. M. J. Swaroopan, and N. R. Shanker, "Prediction of Rotor Slot Size Variations in Induction Motor Using Polynomial Chirplet Transform and Regression Algorithms," *Arabian Journal for Science and Engineering*, vol. 48, no. 5, pp. 6099–6109, May 2023, doi: 10.1007/s13369-022-07264-9.
[33] H. D. Nirwana, A. R. Saidy, G. M. Hatta, and A. Nugroho, "Design of a Green City with Lower Carbon Based on Vegetation in Banjarbaru using Sentinel-2," *Journal of Applied Data Sciences*, vol. 5, no. 2, pp. 583–599, May 2024, doi: 10.47738/jads.v5i2.218.
[34] S. P. Suryodiningrat and M. Tarigan, "Machine Learning Based Cyber Attack Detection in Network Systems Using Network Session Behavioral Features," *Journal of Cyber Law*, vol. 2, no. 2, pp. 130–145, Jun. 2026, doi: 10.63913/jcl.v2i2.29.
[35] J. A. Kumar, M. Gowthambigai, N. R. Shanker, and J. Jasper, "Prediction of rotor slot width in induction motor using Dyadic wavelet transform and softmax regression," *International Journal of Emerging Electric Power Systems*, vol. 25, no. 1, pp. 83–95, Feb. 2024, doi: 10.1515/ijeeps-2022-0214.
[36] H. A. Awad, "Deep Learning-Based Digital Twin Framework for Real-Time Water Network Anomaly Detection," *International Journal Research on Metaverse*, vol. 3, no. 3, pp. 180–192, Aug. 2026, doi: 10.47738/ijrm.v3i3.56.
[37] Z. Tashenova, S. Amanzholova, Z. Abdugulova, and E. Nurlybaeva, "Modeling Thermomechanical Effects in Rods with Variable Cross-Section and Local Heat Sources," *Journal of Applied Data Sciences*, vol. 7, no. 3, pp. 1720–1732, Sep. 2026, doi: 10.47738/jads.v7i3.1340.
[38] J. A. Kumar, M. Gowthambigai, N. R. Shanker, and J. Jasper, "Prediction of Rotor Slot Size Variation Through Vibration Signal of Three Phase Induction Motor Using Machine Learning," *Journal of Vibration Engineering and Technologies*, vol. 12, no. 1, pp. 561–574, Jan. 2024, doi: 10.1007/s42417-023-00859-y.
[39] S. A. Ghaffar, "Exploring Thematic Travel Preferences of Global Cities through Agglomerative Hierarchical Clustering for Enhanced Travel Recommendations," *International Journal for Applied Information Management*, vol. 5, no. 4, pp. 155–167, Dec. 2025, doi: 10.47738/ijaim.v5i4.111.
[40] S. Murugesan, "Dynamic Relationship Analysis Between Gas Used and Gas Price in Ethereum Using VAR and Granger Causality Tests," *Journal of Current Research in Blockchain*, vol. 3, no. 2, pp. 80–95, May 2026, doi: 10.47738/jcrb.v3i2.65.
[41] R. K. Padmashini, D. Lakshmi, T. Sasilatha, and J. G. Raman, "Analysis of Vector Controlled 3 Phase Induction Motor for Ev Applications," *Journal of Engineering Science and Technology*, vol. 19, no. 2, pp. 215–224, 2024.
[42] A. Al-Musawi, F. Anayi, and M. Packianather, "Three-phase induction motor fault detection based on thermal image segmentation," *Infrared Physics & Technology*, vol. 104, p. 103140, 2020, doi: 10.1016/j.infrared.2019.103140.
[43] O. Keleş, M. A. Yılmaz, A. M. Tekalp, C. Korkmaz and Z. Doğan, "On the Computation of PSNR for a Set of Images or Video," in *2021 Picture Coding Symposium (PCS)*, Bristol, United Kingdom, 2021, pp. 1-5, doi: 10.1109/PCS50896.2021.9477470.
[44] T. Gopalakrishnan *et al.*, "Data-driven predictive maintenance of induction motors using self-supervised and federated learning on noisy current and vibration signals," *Scientific Reports*, vol. 16, no. 1, p. 16396, Apr. 2026, doi: 10.1038/s41598-026-46550-6.

BIOGRAPHIES OF AUTHORS



Lakshmi Dandapani received the B.E. degree in Electrical and Electronics Engineering from the University of Madras in 1999 and the M.E. degree in Power Systems Engineering from B.S.A. Crescent Engineering College. She is currently a professor in the Department of Electrical and Electronics Engineering, AMET Deemed to be University, Chennai, India. Her research interests include power system operation and control, electrical engineering applications, condition monitoring, and intelligent techniques for engineering systems. She has academic experience in teaching, research, and supervision in electrical and electronics engineering. She can be contacted at email: Lakshmi.d@ametuniv.ac.in.



Kavitha Selvaraj received her postgraduate and doctoral qualifications in electrical engineering. She is currently affiliated with Saveetha Engineering College, Chennai, India. Her academic and research interests include electrical machines and controllers, renewable energy systems, converters, and induction motor fault diagnosis. She has delivered academic talks related to induction motor rotor fault prediction and has research experience in fault detection and condition monitoring of electrical machines. Her work focuses on applying intelligent methods and sensor-based approaches for improving the reliability of electrical motor systems. She can be contacted at email: kavithavishal20@gmail.com.



Malathy Batumalay received the Ph.D. degree in Photonics Engineering from the University of Malaya, Malaysia. She is currently professor at INTI International University, Malaysia, where she serves in the Faculty of Data Science and Information Technology. Her research interests include photonics, fiber optics, fiber sensors, optical sensing, and technology-based intelligent systems. Her previous research has explored the use of fiber-optic sensors for detecting changes in environmental and chemical conditions. She has also been involved in research related to data science, sustainable technologies, and applied technological solutions. She can be contacted at email: malathy.batumalay@newinti.edu.my.



Taqwa Hariguna received the Ph.D. degree from Southern Taiwan University. He is currently a professor in Computer Science at Universitas Amikom Purwokerto, Indonesia. His research interests include management information systems, e-government, software engineering, information systems impact, information technology management, and intelligent computing applications. He has published in areas related to information systems, software development, IT project management, and applied computing. His research work contributes to the development and evaluation of information technology and intelligent systems in organizational and applied contexts. He can be contacted at email: taqwa@amikompurwokerto.ac.id.